Journal of Magnetics 16(1), 6-9 (2011) DOI: 10.4283/JMAG.2011.16.1.006

Spin-Motive Force Caused by Vortex Gyration in a Circular Nanodisk with Holes

Jung-Hwan Moon and Kyung-Jin Lee*

Dept. of Materials Science of Engineering, Korea University, Seoul 137-153, Korea

(Received 1 November 2010, Received in final form 1 December 2010, Accepted 13 December 2010)

Spin-motive force has drawn attention because it contains a fundamental physical property. Spin-motive force creates effective electric and magnetic fields in moving magnetization; a vortex is a plausible system for observing the spin-motive force because of the abrupt profile of magnetization. However, the time-averaged value of a spin-motive force becomes zero when a vortex core undergoes gyroscopic motion. By means of micromagnetic simulation , we demonstrates that a non-zero time-averaged electric field induced by spin-motive force under certain conditions. We propose an experimental method of detecting spin-motive force that provides a better understanding of spin transport in ferromagnetic system.

Keywords : micromagnetic calculation, vortex dynamics, spin-motive force

1. Introduction

Electromotive force (EMF) is generated from the time derivative of a magnetic field, i.e., Faraday's law. It was recently suggested that EMF can arise from the spin of electrons in ferromagnetic materials – this is called spin-motive force [1, 2]. Spin-motive force is a generalized EMF that includes a spin-averaged Berry phase; it is observed when temporal and spatial variations of magnetization, such as domain wall motion and the gyrotropic motion of a magnetic vortex, exist in ferromagnetic materials. It contains fundamental physical quantities in spintronics, such as spin-dependent EMF and additional damping torque caused by magnetization dynamics [3-5]. Thus, investigating spin-motive force requires a suitable modeling system.

Yang *et al*. experimentally observed generalized EMF using domain wall (DW) motion in a nanostrip [6]. A DW exhibits steady stream motion in a magnetic field below a certain threshold (i.e., the Walker breakdown field [7]). Above this threshold, an anti-vortex periodically nucleates at the wire edge and moves transversely in the direction of wire width. A voltage drop occurs in the direction of DW propagation, which depends only on the transformation frequency of the DW. This provides experimental evidence of spin-originated EMF, which is expressed as the cross product of the spatial gradient of magnetization and its time derivative [8-12].

In this sense, the vortex gyration in a nanodisk is suitable for investigating the spin-motive force – it provides a non-zero value of the cross product between the spatial and temporal changes of the magnetization. However, vortex gyration is generally a periodic function of time; thus, the time-averaged electric field caused by spin-motive force will be zero, which makes it difficult to detect using DC measurements. Recently, Silva *et al*. showed the possibility of breaking the periodicity of vortex gyration by introducing defects (small holes) via a vortex core reversal in a nanodisk [13]. When a vortex core undergoes a modified gyroscopic motion from the introduction of defects, it is possible to obtain a non-zero DC electric field, which opens a way to detecting spin-motive force.

2. Micromagnetic Simulation

We performed micromagnetic simulation with the Landau-Lifshitz-Gilbert (LLG) equation:

$$\frac{\partial \mathbf{M}}{\partial t} = -\gamma \mathbf{M} \times \mathbf{H}_{eff} + \frac{\alpha}{M_S} \mathbf{M} \times \frac{\partial \mathbf{M}}{\partial t} \quad (1)$$

where $\mathbf{M}$ is the local magnetization vector, γ is the gyromagnetic ratio (1.76×10^7 $\mathrm{sec^{-1}Oe^{-1}}$), $\mathbf{H}_{eff}$ is the effective field, consisting of the exchange, magnetostatic, and external field, M_S is the saturation magnetization, and α is the Gilbert damping constant. An alternating current (ac)

*Corresponding author: Tel: +82-2-3290-3289
Fax: +82-2-928-3584, e-mail: kj_lee@korea.ac.kr

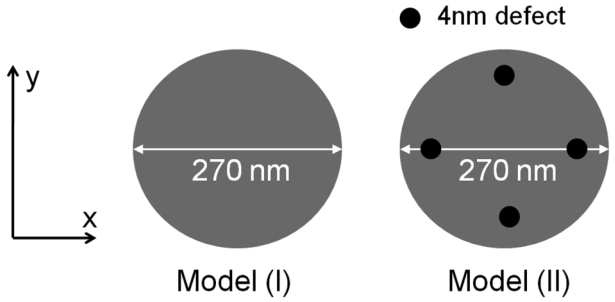

Fig. 1. Schematic illustration of Model I and Model II.

external magnetic field with a frequency of 605.5 MHz is applied along the x-axis. A circular Permalloy disk was assumed, with a 20 nm thickness and diameter of 270 nm. The cell size is $2 \times 2 \times 20$ nm^3 and standard material parameters of Permalloy are used: an exchange constant (A) of 1.3×10^{-6} erg/cm^2 and Gilbert damping constant (α) of 0.01. 605.5 MHz is the resonant frequency of this system, as determined by micromagnetic simulation. We investigated ac magnetic field-induced vortex dynamics in two different systems – Models (I) and (II). Model (I) has no defects (holes) in the nanodisk, whereas Model (II) has four. The holes, sized 4, 12, and 20 nm, are designed to create collisions with a vortex core during gyrotropic motion (Fig. 1).

3. Results and Discussion

Equation (2) describes the *i*th component of the electric field induced by spin-motive force [5-11, 13]:

$$E_i \equiv -\partial_i V^S - \partial_t A_i^S = \pm(\hbar/2e)(\partial_t \mathbf{m} \times \partial_i \mathbf{m}) \cdot \mathbf{m} \qquad (2)$$

where A^s is the vector potential, V^s is the scalar potential, **m** is the unit vector of magnetization, and ± stands for spin-up and spin-down bands. When we calculate the electric field using Eq. (2), the ratio of spin-up to spin-down is assumed to be 0.7 for Permalloy [14, 15].

As shown in Eq. (2), the electric field induced by spin-motive force is given by the product of the spatial gradient of magnetization and its time derivative. Because of the abrupt change in magnetization near a vortex core, the spatial gradient of magnetization should be large. The time derivative of magnetization (= velocity of a vortex core) is a few hundred m/s when a vortex core undergoes gyrotropic motion. Thus, the electric field induced by spin-motive force should originally be large in the vortex state. As a result, it is a suitable system for investigating spin-motive force.

When a vortex core undergoes gyrotropic motion, the time derivative of magnetization, i.e., the velocity of a vortex core along the x- or y-axis, periodically changes its sign because a vortex core follows a circular trajectory. If the sign of the x-axis (or y-axis) velocity of a vortex core is positive in the first half cycle, it becomes negative in the second half cycle. If we ignore a small change of the spin texture of the vortex during gyration, the induced electric field then shows periodic oscillation because only the time derivative of magnetization changes its sign. Thus, the time-averaged electric field is significantly diminished.

When a vortex core collides with a hole, the polarity of a vortex core is reported to switch after collision. The polarity of a vortex core in both field- [16] and current-driven vortex dynamics governs the direction of gyrotropic motion [17]. Thus, hole-vortex collisions can change the trajectory of a vortex core and the sign of core velocity along the x-axis (y-axis).

The modeling examines the dynamics of a vortex core for rectangular defects with varied sizes (4, 12, and 20 nm) and locations. The hole position is placed on an arbitrary circle whose radius is half that of the nanodisk. First, we change the hole size to examine the relation between hole size and core reversal – vortex core reversal was observed only for a 4 nm hole. When a vortex core rotates clockwise (or anti-clockwise), the direction of the gyration becomes anti-clockwise (or clockwise) after collision with the hole with the emission of spin waves. In the case of 12 and 20 nm holes, a vortex core pinned after collision with the hole. Second, we assumed two holes and examined repetitive reversal. By adjusting the amplitude of the external field and position of holes, it is possible to limit vortex gyration between two holes. In this case, both the spatial and temporal derivatives change their sign. The electric field induced by spin-motive force, given by the product of the spatial and temporal derivatives, does not change its sign.

Model (II) assumes four, 4 nm holes at intervals of 90 degrees. An ac magnetic field of 40 Oe with a frequency of 605.5 MHz is applied to Models (I) and (II) along the x-axis. A vortex core is originally located at the center of a nanodisk. After applying the external magnetic field, a vortex core moved in the opposite direction of the external field; its trajectory followed a spiral. Finally, in Model (I), it reached a circular trajectory with an equilibrium radius of gyration. In the case of Model (II), the trajectory of a vortex core was not circular. Because the holes are positioned such that they will collide with a vortex core during gyration, a vortex core collided with the holes repeatedly. Whenever a collision occurred, a vortex core changed both its polarity and direction of gyration. Thus, the trajectory of a vortex core made a quadrant circle instead of a circular shape. We observed

several consecutive reversals of a vortex core. However, the collisions between the hole and a vortex core were not endless. We attributed this limitation on the collisions to energy dissipation due to the generation of spin waves.

There are various methods of determining the position of a vortex core, such as searching the maximum m_z (z-component of magnetization) value. However, because of the heavy radiation of spin waves when a vortex core reverses, it is very difficult to determine the position of a vortex core by searching the m_z component. Another way to determine the position of a vortex core is to use spatially averaged m_x and m_y. When a vortex core is located at the center of a nanodisk, the value of averaged m_x ($<m_x>$) and averaged m_y ($<m_y>$) are zero due to the symmetric configuration of the magnetic vortex. When a vortex core deviates from the center of a nanodisk, the value of an $<m_x>$ (or $<m_y>$) also deviates from zero, corresponding to radius of gyration. Thus, we can roughly determine the position of a vortex core by plotting $<m_x>$ versus $<m_y>$. The inset of Fig. 2 shows $<m_y>$ as a function of $<m_x>$ of a nanodisk from 0 to 20 ns for Model (II), which describes the trajectory of a vortex core. A vortex core began to show gyration and a circular trajectory; however, during the short range (in the case of Model II, 9-11 ns) a vortex core showed pendulum motion between the holes. Fig. 2 shows the position of a vortex core from 8-10 ns; an open circle describes the position of a vortex core at every 50 ps. After the first and second collisions, the trajectory of a vortex core maintained its radius – it could potentially collide with the hole and change its polarity. However, after the third collision the trajectory of a vortex core did not overlap the position of the hole. Thus, the trajectory of a vortex core is circular until its radius becomes large enough to reach the holes.

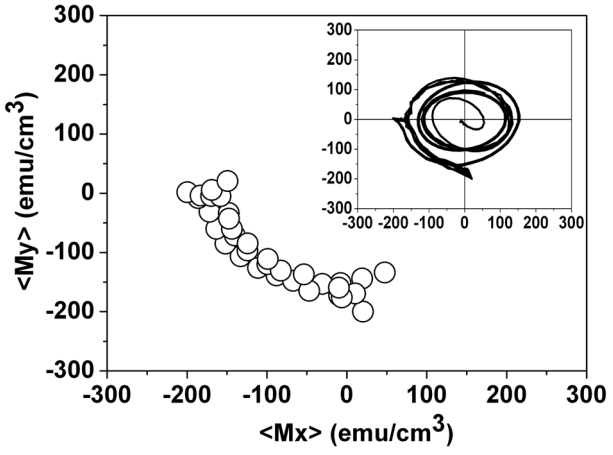

Fig. 2. The position of a vortex core is plotted every 50 ps during pendulum motion (0-11 ns). The inset shows the trajectory of a vortex core for 20 ns in the case of Model II.

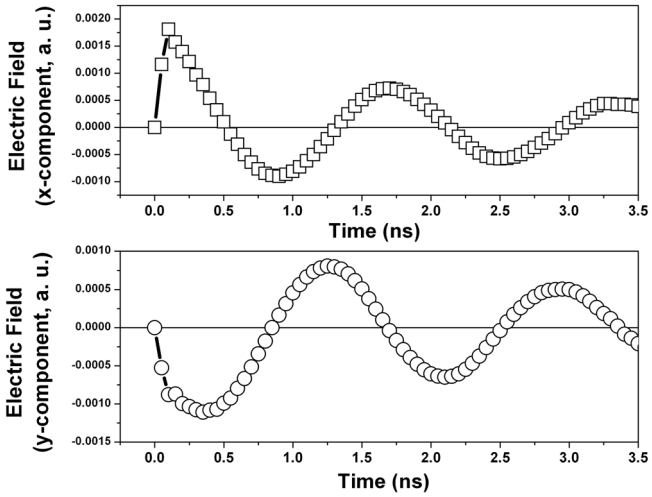

Fig. 3. x- and y-components of the spin-dependent electric field of Model I.

The quadrant-circle-shaped trajectory is only observed for a short time, although a vortex core is expected to continue running between holes. Because of the spin wave, which is generated by core reversal, the radius of the trajectory becomes small due to the energy loss. A vortex core could not collide with a hole after a series of collisions even if more energy is provided by the external magnetic field. However, after a time, the trajectory of a vortex core regains the potential of colliding with the defect by obtaining sufficient energy from the resonant ac magnetic field.

For Model (I), the electric field induced by spin-motive force is calculated using Eq. (2), as shown in Fig. 3, which shows a sinusoidal wave as a function of the time. Because the sign of electric field changed repeatedly, the time-averaged electric field becomes zero, as predicted.

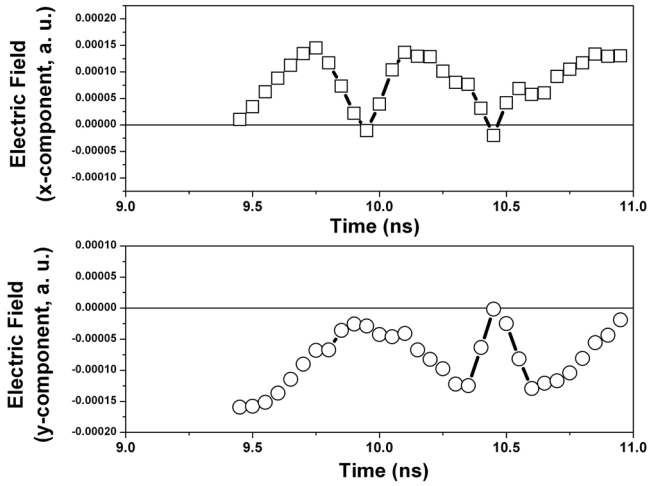

Fig. 4. x- and y-components of the spin-dependent electric field of Model II.

However, in Model (II), a vortex core changed both the polarity and the sign of velocity when it collided with a hole. The sign of the electric field can be conserved in this case; thus, a non-zero, time-averaged electric field could be obtained, as shown in Fig. 4.

4. Conclusion

Using micromagnetic simulation, spin-motive force was examined in a circular nanodisk with defects. The polarity of a vortex core can be controlled using the defects; thus, we can design a vortex core trajectory suitable for detection of spin-motive force. By introducing appropriately sized defects in a nanodisk (Model (II)), the detection of spin-motive force could be achieved. Thus, it is an important tool for studying the relationship between the charge and spin transports in a ferromagnetic system.

Acknowledgement

This work was supported by the KOSEF through the NRL program, funded by the Korean Ministry of Education, Science and Technology (Project No. M10600000198-06J0000-19810) and the DRC Program funded by the KRCF.

References

[1] S. E. Barnes and S. Maekawa, Phys. Rev. Lett. **98**, 246601 (2007).
[2] S. E. Barnes, J. Magn. Magn. Mater. **310**, 2035 (2007).
[3] S. Zhang and S. S.-L. Zhang, Phys. Rev. Lett. **102**, 086601 (2009).
[4] J.-H. Moon, S.-M. Seo, and K.-J. Lee, IEEE Trans. Magn. **46**, 2167 (2010).
[5] S.-I. Kim, J.-H. Moon, W. Kim, and K.-J. Lee, Curr. Appl. Phys. **11**, 61 (2011).
[6] S. A. Yang, G. S. D. Beach, C. Knutson, D. Xiao, Q. Niu, M. Tsoi, and J. L. Erskine, Phys. Rev. Lett. **102**, 067201 (2009).
[7] N. L. Schryer and L. R. Walker, J. Appl. Phys. **45**, 5406 (1974).
[8] W. M. Saslow, Phys. Rev. B **76**, 184434 (2007).
[9] S. A. Yang, D. Xiao, and Q. Niu, arXiv: 0709.1117v3 (unpublished).
[10] Y. Tserkovnyak and M. Mecklenburg, Phys. Rev. B **77**, 134407 (2008).
[11] R. A. Duine, Phys. Rev. B **77**, 014409 (2008).
[12] J. Shibata and H. Kohno, Phys. Rev. Lett. **102**, 086603 (2009).
[13] R. L. Silva, A. R. Pereira, R. C. Silva, W. A. Moura-Melo, N. M. Oliveira-Neto, S. A. Leonel, and P. Z. Coura, Phys. Rev. B **78**, 054423 (2008).
[14] J. Ohe and S. Maekawa, J. Appl. Phys. **105**, 07C706 (2009).
[15] J. Ohe, S. E, Barnes, H.-W. Lee, and S. Maekawa, Appl. Phys. Lett. **95**, 123110 (2009).
[16] B. Van Waeyenberge, A. Puzic, H. Stoll, K. W. Chou, T. Tyliszczak, R. Hertel, M. Fähnle, H. Brückl, K. Rott, G. Reiss, I. Neudecker, D. Weiss, C. H. Back, and G. Schütz, Nature **444**, 461 (2006).
[17] K. Yamada, S. Kasai, Y. Nakatani, K. Kobayashi, H. Kohno, A. Thiaville, and T. Ono, Nat. Mater. **6**, 270 (2007).